



Large reversible magnetocaloric effect in RMn_2 ($R = Tb, Dy, Ho, Er$) compounds



Wenliang Zuo*, Fengxia Hu, Jirong Sun, Baogen Shen*

State Key Laboratory for Magnetism, Institute of Physics, Chinese Academy of Sciences, Beijing 100190, People's Republic of China

ARTICLE INFO

Article history:

Received 8 February 2013

Received in revised form 18 March 2013

Accepted 20 March 2013

Available online 10 April 2013

Keywords:

RMn_2 compounds

Magnetocaloric effect

Magnetic entropy change

Magnetic refrigeration capacity

ABSTRACT

Magnetocaloric effect (MCE) of RMn_2 ($R = Tb, Dy, Ho, Er$) compounds are investigated. $TbMn_2$ and $DyMn_2$ crystallize in cubic Laves phase structure (C15 type), whereas $HoMn_2$ and $ErMn_2$ crystallize in hexagonal Laves phase structure (C14 type). For $TbMn_2$ compound, the field-induced metamagnetic transition accompanying a spontaneous cell volume expansion is observed (inverse MCE), which leads to a large positive value ($8.3 \text{ J kg}^{-1} \text{ K}^{-1}$) of magnetic entropy change around 36 K under the field change of 0–1 T, while the maximal values of magnetic entropy change (ΔS_M) and the refrigerant capacity (RC) for other RMn_2 ($R = Dy, Ho, Er$) compounds are -15.7 , -18.4 , $-25.5 \text{ J kg}^{-1} \text{ K}^{-1}$ and 403.6, 404.3, 316.0 J kg^{-1} around their T_C with negligible thermal and magnetic hysteresis loss for the field change of 0–5 T, respectively. The results suggest that RMn_2 ($R = Dy, Ho, Er$) may be appropriate candidates for magnetic refrigerant working at low temperature region 10–80 K.

© 2013 Elsevier B.V. All rights reserved.

1. Introduction

Investigations of the magnetocaloric effect (MCE) have attracted a great deal of attention owing to the potential applications in magnetic refrigerators [1–5]. The MCE is related to the isothermal magnetic entropy change (ΔS_M) or the adiabatic temperature change (ΔT_{ad}) of a material when exposed to a varying magnetic field. The large values of ΔS_M and ΔT_{ad} are considered to be the most important requirements. In addition, larger refrigeration capacity (RC) without thermal and magnetic hysteresis loss favors efficiency in refrigeration cycles.

During the last few years, RTM_2 ($R = \text{rare earth}, TM = \text{Ni, Co, Al}$) compounds have been considered to be the potential magnetic refrigerant materials working at temperature region of 10–120 K [6–13]. Among these compounds, most of them crystallize in $MgCu_2$ -type cubic structure. Ni and Al atoms carry no-magnetic moment and Co magnetic moment varies between 0–1 μ_B [13–16]. Compared with these compounds, RMn_2 system crystallizes in cubic Laves phase structure (C15 type) or hexagonal Laves phase structure (C14 type) depending on the rare earth element and annealing temperature [16,17]. The magnetic structure is depending on the competitive of magnetic interaction come from Mn–Mn, R–R and R–Mn, furthermore, the interaction is antiferromagnetic between Mn moments but ferromagnetic coupling between R moments. In other words, the magnetic structure and local magnetic

moment of RMn_2 is determined by the lattice constant (the distance of Mn–Mn, R–R and R–Mn) rather than the type of Laves Phase [18,19]. Therefore, the local Mn moment is about 3 μ_B when the lattice parameter is larger than a critical value $a \approx 7.5 \text{ \AA}$ and decrease from about 2.0 μ_B in C14– $GdMn_2$ to almost 0 μ_B in C15– $ErMn_2$ at 4.2 K with increasing the atomic number of rare earth. The more detail description can consult those papers [18–20]. The larger magnetic moment of Mn atom possibly makes RMn_2 compounds show better magnetocaloric effect than that of RTM_2 compounds. Furthermore, the phase transition temperature of RMn_2 compounds locates at the range of 10–80 K. Therefore, the RMn_2 compounds possibly become another potential magnetic refrigerant material system for the gas liquefiers.

In this paper we investigated the MCE of RMn_2 ($R = Tb, Dy, Ho, Er$) compounds. The large MCE is observed in RMn_2 compounds. Furthermore, the very weak field-induced metamagnetic transition behaviors make RMn_2 ($R = Dy, Ho, Er$) compounds exhibit a second-order metamagnetic character. The large refrigeration capacity and low hysteresis loss indicate that RMn_2 ($R = Dy, Ho$) compounds can be potential candidates of magnetic refrigerant working at low temperature region of 10–80 K.

2. Experiments

The RMn_2 ($R = Tb, Dy, Ho, Er$) compounds were prepared by arc-melting in a high purity argon atmosphere. The purities of starting materials were better than 99.9%. The ingots were melted three times to ensure homogeneity and then annealed at 1073 K for 7 days under argon atmosphere and then rapidly quenched to room temperature. The phase structure was examined at room temperature by the X-ray powder diffraction with $Cu K\alpha$ radiation. The Rietveld refinements were carried out for determination of lattice parameters. Magnetizations were measured

* Corresponding authors. Tel.: +86 01082649251 (W. Zuo), +86 01082648082 (B. Shen).

E-mail addresses: wzuo@iphy.ac.cn (W. Zuo), shenbg@aphy.iphy.ac.cn (B. Shen).

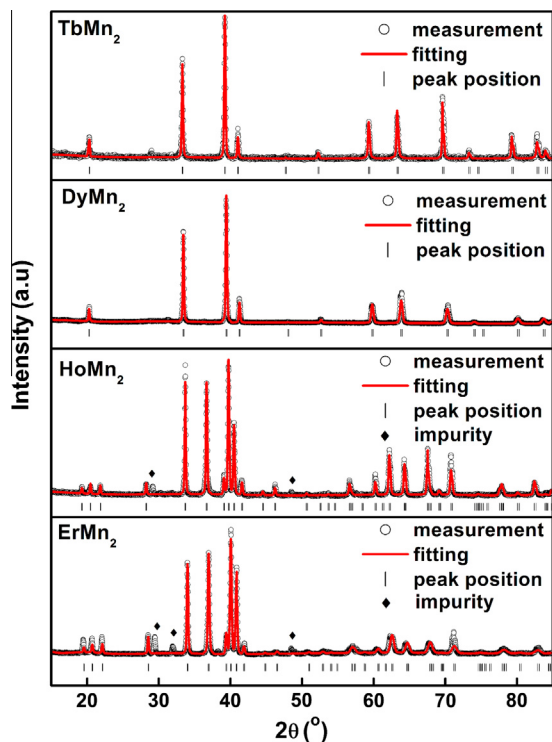


Fig. 1. The measured and refined powder X-ray diffraction (XRD) patterns of RMn_2 ($R = Tb, Dy, Ho, Er$) compounds at room temperature.

Table 1

The lattice parameters and main refinement factor of RMn_2 ($R = Tb, Dy, Ho, Er$) compounds at room temperature.

RMn_2	a (Å)	b (Å)	c (Å)	v (Å ³)	R_{wp} (%)
$R = Tb$	7.648	7.648	7.648	447.487	10.45
$R = Dy$	7.570	7.570	7.570	433.815	9.36
$R = Ho$	5.322	5.322	8.682	212.938	13.02
$R = Er$	5.310	5.310	8.676	211.852	14.91

as functions of temperature and magnetic field by using a commercial superconducting quantum interference device (SQUID) magnetometer, Model MPMS-7 from Quantum Design Inc. The temperature dependences of magnetizations were measured in both zero field-cooled (ZFC) and field-cooled (FC) processes. In the ZFC measurement, the initial field was set to zero when cooling the sample from 300 K to 2 K, the magnetization was measured with a magnetic field of 0.01 T while heating the sample from 2 K to 300 K, and the FC measurement is to measure the magnetization under a same magnetic field of 0.01 T when cooling the sample from 300 K to 2 K.

3. Results and discussion

Fig. 1 shows the measured and refined powder X-ray diffraction (XRD) patterns of RMn_2 ($R = Tb, Dy, Ho, Er$) compounds at room temperature. $TbMn_2$ and $DyMn_2$ compounds crystallize primarily in the $MgCu_2$ -type cubic Laves phase structure (C15-type, Space group $Fd\bar{3}m$, number 227) with minor impurity (R_2O_3). Whereas $HoMn_2$ and $ErMn_2$ compounds primarily crystallize in the $MgZn_2$ -type hexagonal Laves phase structure (C14-type, Space group $P63/mmc$, number 194) with minor impurities (mixture of R_2O_3 and R_6Mn_{23}). The lattice parameters were calculated by the refining XRD data as shown in Table 1. The results agree well with the previous reports [16,18].

Fig. 2 shows the temperature dependences of zero-field-cooled (ZFC) and field-cooled (FC) magnetizations for RMn_2 ($R = Tb, Dy, Ho, Er$) compounds in a magnetic field of 100 Oe. It can be seen that both ZFC and FC curves for $TbMn_2$ show a peak at the temperature between 40 K and 50 K, corresponding to an antiferromagnetic (AFM) to paramagnetic (PM) phase transition at T_N [21]. Furthermore, a thermal hysteresis of about 7 K between ZFC and FC curves below T_N is observed. This generally is the character of thermal-induced first-order magnetic transition. Many groups have demonstrated that the first-order magnetic phase transition for $TbMn_2$ occurs accompanying a spontaneous cell volume expansion which is calculated to be about 1.68% [21–24]. With the temperature further decrease, below 35 K, another phase transition occurs. This transition is not homogeneous but a multiphase transition. The phase consists mainly of two magnetic structures. One is AFM order and the other one is ferromagnetic (FM) order [23–25]. Furthermore, a weak splitting between the ZFC and FC measurement curves of $TbMn_2$ is observed below the transition temperature T_C .

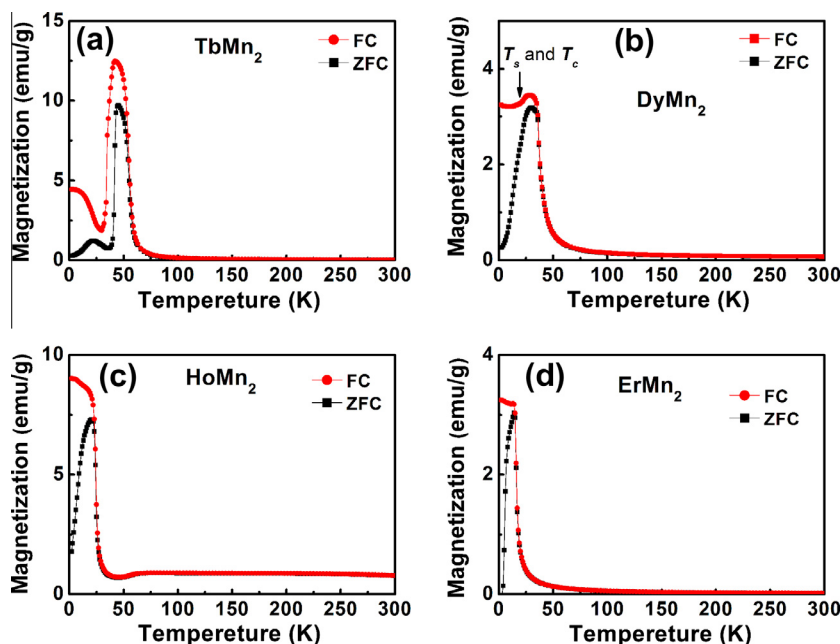


Fig. 2. The temperature dependences of zero-field-cooled (ZFC) and field-cooled (FC) magnetizations for RMn_2 ($R = Tb, Dy, Ho, Er$) compounds in a magnetic field of 100 Oe.

Table 2

The magnetic ordering temperature (T_0), maximum values of ΔS_M and RC under the field changes of 0–2 and 0–5 T for RMn_2 ($R = \text{Gd, Tb, Dy, Ho, Er}$) and some potential magnetic refrigerant materials RTM_2 ($R = \text{rare earth, TM} = \text{Ni, Co, Al}$).

Material	T_0 (K)	$-\Delta S_M$ ($\text{J kg}^{-1}\text{K}^{-1}$)	RC (J kg^{-1})		Refs.
			0–2 T	0–5 T	
GdMn ₂	110	–	3.1	–	150 ^a [42]
TbMn ₂	45	6.4	11.9	99	204 This work
DyMn ₂	36	7.6	15.7	127	404 This work
HoMn ₂	23	10	18.4	130	404 This work
ErMn ₂	16	13.4	25.5	100	316 This work
DyAl ₂	60	9.2	17	236 ^a	600 ^a [10]
HoAl ₂	32	–	29 ^b	–	– [6]
ErAl ₂	13	22	37	150 ^a	470 ^a [10]
HoCo ₂	78	20	23	130 ^a	260 ^a [12]
ErCo ₂	35	28	33	100 ^a	270 [13]
DyNi ₂	21	10.7	21	110 ^a	350 ^a [9]
HoNi ₂	13	–	34	–	300 ^a [9]
ErNi ₂	7	12.3	19.6	96 ^a	235 ^a [9]

^a The RC values are estimated from the temperature dependences of ΔS_M in the reference literatures.

^b The theoretical calculated values.

The phenomenon of splitting was also reported for some intermetallic compounds by other authors [26,27]. The ZFC case generally is prone to a random domain configuration below T_C , whereas the FC case leads to preferred orientation of the spins along the external field direction. Therefore the magnetization is smaller in the ZFC case than FC case. Therefore, the other RMn_2 ($R = \text{Dy, Ho, Er}$) compounds also show a splitting between the ZFC and FC curves below the transition temperature T_C , which are about 36 K, 23 K, and 16 K for RMn_2 ($R = \text{Dy, Ho, Er}$) (see Table 2), respectively, close to the reports [16–18]. Moreover, a decrease in the FC curve for DyMn₂ is also observed at around 20 K (see the arrows in Fig. 2b), which is deemed to be existence of ferrimagnetic (FIM) coupling between Dy and Mn moments by Malik et al. [17]. However, Talik et al. indicated that it is a spin reorientation transition

temperature [28]. Actually, weak spin reorientation transition at $T_S \sim 15$ K and FIM coupling between Dy and Mn moments at T_C below 20 K exist together (see Fig. 6 of Ref. [28]).

Fig. 3a and b show the magnetization (M) isotherms of TbMn₂ compound measured with different temperature steps in a temperature range of 28–69 K. To investigate the magnetic reversibility, the M – H curves were measured in field increasing and decreasing modes. At 28 K, the M – H curve shows an obvious hysteresis loss with the increasing and decreasing field, and the hysteresis become smaller and smaller with increasing the temperature until the hysteresis almost disappear at the temperature above 40 K. Moreover, an obvious metamagnetic transition is observed in Fig. 3a. The critical field (B_C) required for metamagnetic transition is estimated. The value of B_C , defined as the maximum of dM/dH – H curve, is found to be about 2 T at 28 K for TbMn₂. With the temperature further increasing, the isothermal M – H curves exhibit a FM nature and a PM state at the temperature lower and much higher than T_N , respectively (see Fig. 3b). In addition, a strong curvature is observed in the M – H curves with the temperature above T_N at low fields, which is also observed in other intermetallic compounds [29–31], indicates that short-range FM correlations are existence in the PM state for TbMn₂ compound. Fig. 3c and d show the Arrott plots of TbMn₂. According to the Banerjee criterion [32], a magnetic transition is the first-order when the slope of Arrott curves is negative, whereas it will be the second-order when the slope is positive. The S-shaped (negative slope) Arrott curves (see Fig. 3c) indicate that the field-induced AFM–FM metamagnetic transition is of first-order in nature, while the positive slope above T_N indicates a characteristic of second-order FM–PM transition (see Fig. 3d).

Fig. 4a–c show the magnetization isotherms of RMn_2 ($R = \text{Dy, Ho, Er}$) compounds measured with different temperature steps in a temperature range of 24–65 K, 12–55 K and 4–50 K, respectively. Measurement was in the field increasing and decreasing modes and very weak hysteresis was observed for all the RMn_2 ($R = \text{Dy, Ho, Er}$) compounds, furthermore, this result agrees with other authors' reports [28,33,34]. For clarity, here we didn't show the curves measured in field decreasing modes. It is obviously seen that all RMn_2 ($R = \text{Dy, Ho, Er}$) compounds exhibit a FM behavior when the temperature is lower than the corresponding transition temperature and the applied field large is larger than 1 T. However,

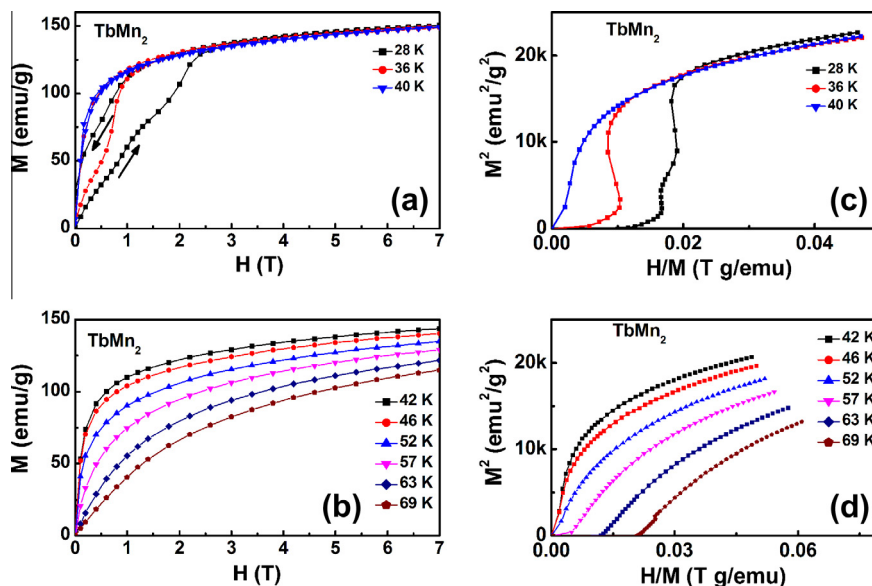


Fig. 3. (a and b) The magnetization isotherms of TbMn₂ compound in a temperature range of 28–69 K. (c and d) the corresponding Arrott curves for TbMn₂ compound.

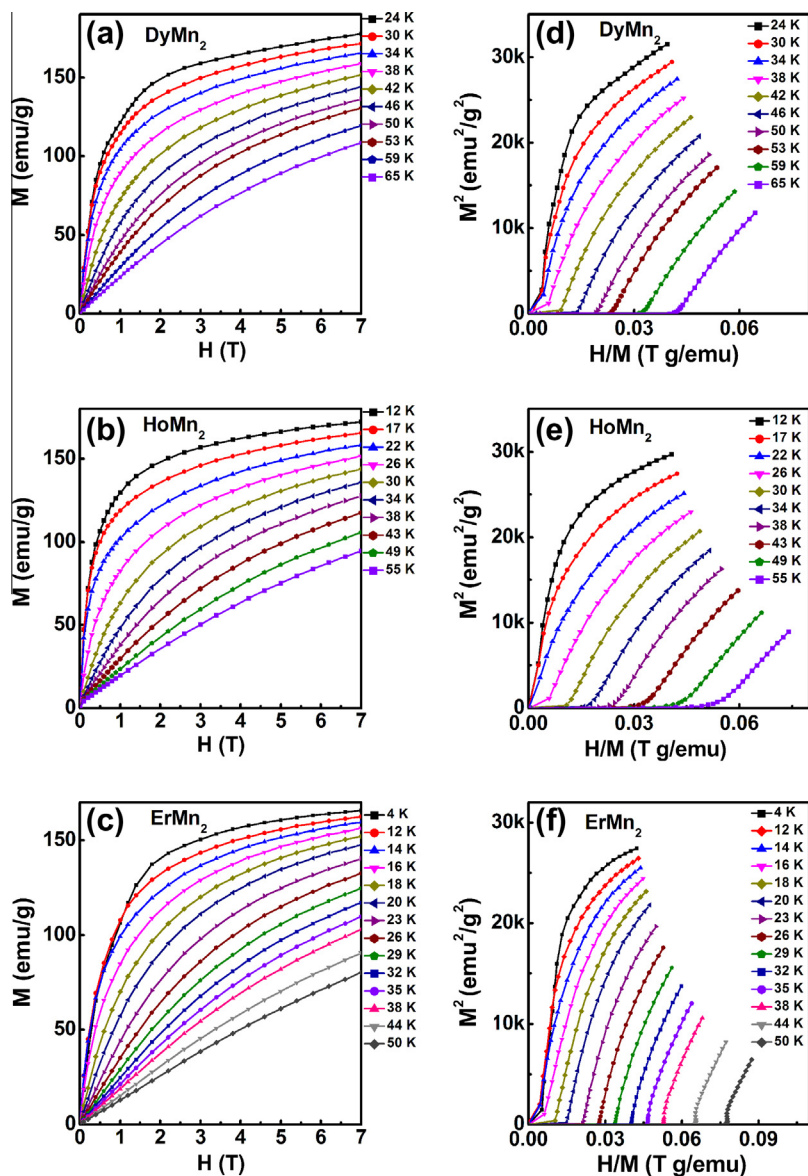


Fig. 4. (a–c) The magnetization isotherms of RMn_2 ($R = Dy, Ho, Er$) compounds with different temperature steps in a temperature range of 24–65 K, 12–55 K and 4–50 K, respectively. (d–f) the corresponding Arrott curves for RMn_2 ($R = Dy, Ho, Er$) compounds.

for $ErMn_2$ single crystals, many authors found that the metamagnetic transition behavior is observed when the magnetization is along both a and b -axes of hexagonal Laves phase structure, while no metamagnetic transition occurred when the magnetization is along the c -axis [16,34]. Therefore, the $ErMn_2$ polycrystalline compound should have a metamagnetic transition behavior, however, which isn't obviously observed in Fig. 4c, can be due to the small critical field B_c (smaller than 1 T). Fig. 4d–f show the Arrott curve of RMn_2 ($R = Dy, Ho, Er$) compounds. An obvious inflexion is observed for $DyMn_2$ and $ErMn_2$ at low temperature region under low field (see the left lower corner of Fig. 4d and f). However, no negative slope can be exhibited in the Arrott curve for those compounds. And thus we deduced that the phase transition for $DyMn_2$ and $ErMn_2$ is more prone to second-order than first-order character [35,36]. For $HoMn_2$, neither inflexion nor negative slope is observed, therefore, the phase transition is second-order magnetic transition. The values of ΔS_M for RMn_2 ($R = Tb, Dy, Ho, Er$) compounds were calculated using the integrated Maxwell relation $\Delta S_M(T, H) = \int_0^H (\partial M / \partial T)_H dH$ and the data is from the magnetization

versus magnetic field on the field increasing modes. Fig. 5 shows the temperature dependences of ΔS_M for different magnetic field changes up to 7 T. For $TbMn_2$ compound, a positive ΔS_M is observed at low temperature as shown in Fig. 5a. The maximum value of ΔS_M reaches $8.3 \text{ J kg}^{-1} \text{ K}^{-1}$ with the field change of 0–1 T. The value is larger than that of most magnetic materials with the inverse magnetocaloric effect, such as $Nd_{0.5}Sr_{0.5}MnO_3$ ($1.5 \text{ J kg}^{-1} \text{ K}^{-1}$) [37], $SmMn_2Ge_2$ ($3.3 \text{ J kg}^{-1} \text{ K}^{-1}$) [38], and $TbSm$ bulk metallic glass ($3.6 \text{ J kg}^{-1} \text{ K}^{-1}$) [39]. Furthermore, the maximum values of ΔS_M are larger than $10 \text{ J kg}^{-1} \text{ K}^{-1}$ with the field changes from 0–2 T to 0–7 T, and the peak height of ΔS_M is not sensitive to the size of the external field while the position of the peak nearly linearly with magnetic field. Generally speaking, this phenomenon is the characterization of first-order phase transition [1], and in here is associated with the field-induced first-order AFM–FM metamagnetic transition accompanying a spontaneous cell volume expansion. Tishin et al. estimated that the lattice entropy change ΔS_{LFO} is $\sim 94 \text{ J kg}^{-1} \text{ K}^{-1}$ for $TbMn_2$ [40], which is about an order of magnitude larger than our observed ΔS_M . The reason is possibly

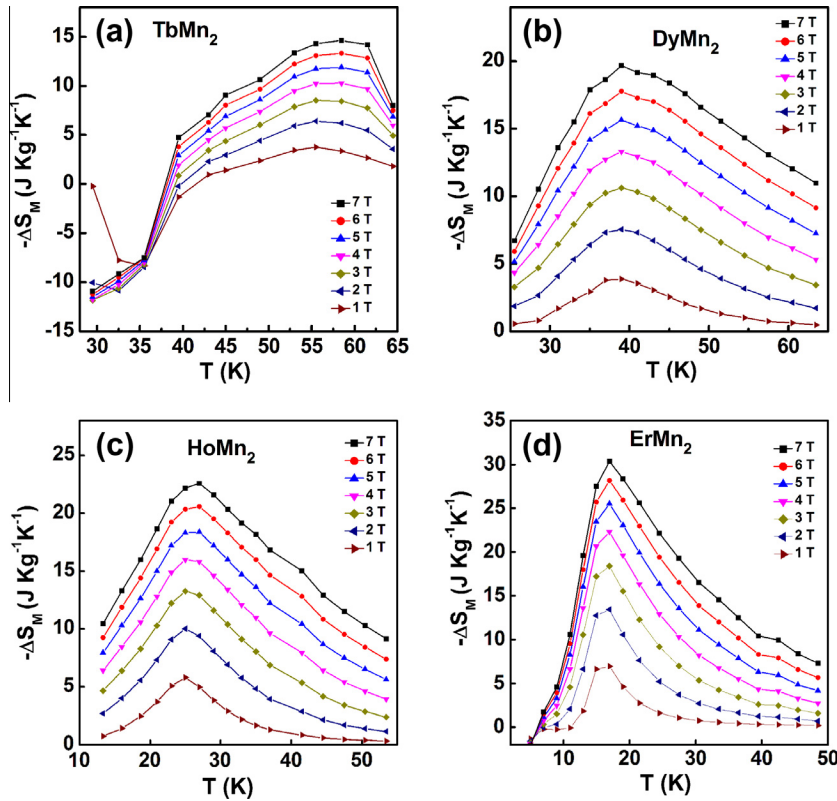


Fig. 5. The temperature dependences of isothermal magnetic entropy change ΔS_M for (a) TbMn_2 , (b) DyMn_2 , (c) HoMn_2 , (d) ErMn_2 compounds.

as follows: One is that such larger ΔS_M is not observed due to the position of ΔS_M peak is smaller than our minimum calculated temperature 30 K. The other is that the estimated ΔS_{LFO} value is incorrect due to the erroneous values of dT_c/dP from other literature data [40]. In addition, the normal magnetocaloric effects (negative value) are also observed in Fig. 5a. The maximum values of ΔS_M for TbMn_2 are -6.4 , -11.9 , and $-14.6 \text{ J kg}^{-1} \text{ K}^{-1}$ around T_N for magnetic field changes of 0–2 T, 0–5 T and 0–7 T, respectively. In comparison, DyMn_2 and HoMn_2 only show the negative values of ΔS_M in the measurement temperature region as shown in Fig. 5b and c. Li et al. indicated that the ΔS_M should appear positive values for the field-induced AFM–FM transition [41]. However, the ΔS_M for DyMn_2 only exhibit the negative values, which is possibly due to the field-induced AIM–FM transition temperature ($\leq 20 \text{ K}$) is smaller than calculated minimum temperature of 26 K (see Fig. 5b). This result is also agreement with the FIM–FM phase transition observed in Fig. 2b but is not observed in Fig. 4a [17,28]. The maximum values of ΔS_M for DyMn_2 and HoMn_2 are -7.6 , -15.7 , $-19.7 \text{ J kg}^{-1} \text{ K}^{-1}$ and -10.0 , -18.4 , $-22.6 \text{ J kg}^{-1} \text{ K}^{-1}$ with the field changes of 0–2 T, 0–5 T and 0–7 T, respectively, which are comparable to those of potential magnetic refrigerant materials RTM_2 ($R = \text{rare earth, TM} = \text{Ni, Co, Al}$) with the a similar phase transition temperature (see Table 2), such as RCO_2 ($R = \text{Ho, Er}$) [12,13], RAL_2 ($R = \text{Dy, Ho, Er}$) [6,10], RNi_2 ($R = \text{Dy, Ho, Er}$) [9]. For ErMn_2 compound, small positive ΔS_M values are observed in the left lower corner of Fig. 5d. The maximum values of ΔS_M reach -13.4 , -25.5 , and $-30.4 \text{ J kg}^{-1} \text{ K}^{-1}$ with the field changes of 0–2 T, 0–5 T and 0–7 T, respectively. It is noted that such giant ΔS_M values are comparable or even much larger than those of RTM_2 magnetic refrigerant materials under the same field changes (see Table 2). The large MCE for ErMn_2 is associated with the weak field-induced metamagnetic transition. Especially for the relatively low magnetic field change of 0–2 T, the values of ΔS_M for HoMn_2 and ErMn_2 are larger than $10 \text{ J kg}^{-1} \text{ K}^{-1}$. It is beneficial to the magnetic refrigera-

tion by using the permanent magnet since a magnetic field of 2 T can be provided by a permanent magnet.

The refrigerant capacity (RC) is another important quality factor of the refrigerant materials and is a measurement of how much heat can be transferred between the cold and hot sinks in one ideal refrigerant cycle, which is defined as $RC = \int_{T_1}^{T_2} |\Delta S_M| dT$, where T_1 and T_2 are the temperatures corresponding to the both sides of the half-maximum value of $|\Delta S_M|$ peak, respectively. For DyMn_2 and HoMn_2 , large RC values of 403.6 J kg^{-1} and 404.3 J kg^{-1} are obtained for a magnetic field change of 0–5 T, respectively, which are comparable or even larger than those traditional RTM_2 ($R = \text{rare earth, TM} = \text{Ni, Co, Al}$) magnetic refrigerant materials, such as RCO_2 ($R = \text{Ho, Er}$) [12,13], RNi_2 ($R = \text{Dy, Ho, Er}$) [9]. The magnetic ordering temperature (T_0), maximum values of ΔS_M and RC under the field changes of 0–2 and 0–5 T for RMn_2 ($R = \text{Gd, Tb, Dy, Ho, Er}$) and RTM_2 ($R = \text{rare earth, TM} = \text{Ni, Co, Al}$) are shown in Table 2. The large ΔS_M and RC for RMn_2 ($R = \text{Dy, Ho, Er}$) compounds with negligible thermal and magnetic hysteresis loss indicate that those compounds probably are promising candidates for practical application in low-temperature magnetic refrigeration.

4. Conclusions

The magnetic properties and MCEs for RMn_2 ($R = \text{Tb, Dy, Ho, Er}$) compounds are studied. For TbMn_2 , the large positive value ΔS_M , which is result from the field-induced first-order magnetic transition, reaches $8.3 \text{ J kg}^{-1} \text{ K}^{-1}$ with the field change of 0–1 T. For other RMn_2 ($R = \text{Dy, Ho, Er}$) compounds, the maximum values of ΔS_M reaches -15.7 , -18.4 , and $-25.5 \text{ J kg}^{-1} \text{ K}^{-1}$ around transition temperature with negligible thermal and magnetic hysteresis loss under a magnetic field change of 0–5 T, respectively. Especially the refrigerant capacity RC for DyMn_2 and HoMn_2 compounds are larger than 400 J kg^{-1} with a magnetic field change of 0–5 T. The

results suggest that RMn_2 ($R = Tb, Dy, Ho, Er$) compounds probably are promising candidates for magnetic refrigerants working at low temperature region 10–80 K.

Acknowledgments

This work was supported by the National Natural Science Foundation of China, the Hi-Tech Research and Development program of China, the Key Research Program of the Chinese Academy of Sciences, and the National Basic Research of China.

References

- [1] A. Smith, C.R.H. Bahl, R. Bjørk, K. Engelbrecht, K.K. Nielsen, N. Pryds, *Adv. Energy Mater.* 2 (2012) 1288–1318.
- [2] K.A. Gschneidner Jr, V.K. Pecharsky, A.O. Tsokol, *Rep. Prog. Phys.* 68 (2005) 1479–1539.
- [3] B.G. Shen, J.R. Sun, F.X. Hu, H.W. Zhang, Z.H. Cheng, *Adv. Mater.* 21 (2009) 4545–4564.
- [4] N.A. de Oliveira, P.J. von Ranke, *Phys. Rep.* 489 (2010) 89–159.
- [5] O. Gutfleisch, M.A. Willard, E. Brück, C.H. Chen, S.G. Sankar, J.P. Liu, *Adv. Mater.* 23 (2011) 821–842.
- [6] P.J. von Ranke, N.A. de Oliveira, M.V. Tovar Costa, E.P. Nobrega, A. Caldas, I.G. de Oliveira, *J. Magn. Magn. Mater.* 226–230 (2001) 970–972.
- [7] P.J. von Ranke, D.F. Grangeia, A. Caldas, N.A. de Oliveira, *J. Appl. Phys.* 93 (2003) 4055–4059.
- [8] N.A. de Oliveira, P.J. von Ranke, M.V. Tovar Costa, A. Troper, *Phys. Rev. B* 66 (2002) 094402.
- [9] E.J.R. Plaza, V.S.R. de Sousa, M.S. Reis, P.J. von Ranke, *J. Alloy. Comp.* 505 (2010) 357–361.
- [10] P.J. von Ranke, V.K. Pecharsky, K.A. Gschneidner Jr, *Phys. Rev. B* 58 (1998) 12110–12116.
- [11] P.J. von Ranke, E.P. Nóbrega, I.G. de Oliveira, A.M. Gomes, R.S. Sarthour, *Phys. Rev. B* 63 (2001) 184406.
- [12] T. Tohei, H. Wada, *J. Magn. Magn. Mater.* 280 (2004) 101–107.
- [13] N.K. Singh, K.G. Suresh, A.K. Nigam, S.K. Malik, A.A. Coelho, S. Gama, *J. Magn. Magn. Mater.* 317 (2007) 68–79.
- [14] F. Pourarian, *J. Phys. Chem. Solids* 41 (1980) 123–127.
- [15] D. Givord, F. Givord, D. Gignoux, W.C. Koehler, R.M. Moon, *J. Phys. Chem. Solids* 37 (1976) 567–569.
- [16] Y. Makihara, Y. Andoh, Y. Hashimoto, H. Fujii, M. Hasuo, T. Okamoto, *J. Phys. Soc. Jpn.* 52 (1983) 629–636.
- [17] S.K. Malik, W.E. Wallace, *J. Magn. Magn. Mater.* 24 (1981) 23–28.
- [18] K. Inoue, Y. Nakamura, A.V. Tsvyashchenko, L. Fomicheva, *J. Phys. Soc. Jpn* 64 (1995) 2175–2182.
- [19] M. Shiga, *J. Magn. Magn. Mater.* 129 (1994) 17–25.
- [20] R. Ballou, *Can. J. Phys.* 79 (2001) 1475–1485.
- [21] S. Mondal, R. Cywinski, S.H. Kilcoyne, B.D. Rainford, C. Ritter, *Physica B* 180–181 (1992) 606–608.
- [22] R. Ballou, J. Deportes, R. Iemaire, P. Rouault, and J. L. Soubeyrou, *J. Magn. Magn. Mater.* 90–91 (1990) 559–560.
- [23] P.J. Brown, B. Ouladdiaf, R. Ballou, J. Deportes, A.S. Markosyan, *J. Phys.: Condens. Matter* 4 (1992) 1103–1113.
- [24] M.R. Ibarra, C. Marquina, L. García-Orza, A. del Moral, *Solid State Commun.* 87 (1993) 695–698.
- [25] R. Ballou, B. Ouladdiaf, P.J. Brown, M.D. Nunez Regueiro, C. Lacroix, *Phys. Rev. B* 45 (1992) 3158–3160.
- [26] C. Ritter, S.H. Kilcoyne, R. Cywinski, *J. Phys.: Condens. Matter* 3 (1992) 727–738.
- [27] E. Duman, M. Acet, I. Dincer, A. Elmali, Y. Elerman, *J. Magn. Magn. Mater.* 309 (2007) 40–53.
- [28] E. Talik, M. Kulpa, T. Mydlarz, J. Kusz, H. Böhm, *J. Alloy. Comp.* 308 (2000) 30–37.
- [29] N.K. Singh, K.G. Suresh, R. Nirmala, A.K. Nigam, S.K. Malik, *J. Appl. Phys.* 101 (2007) 093904.
- [30] P. Arora, P. Tiwari, V.G. Sathe, M.K. Chattopadhyay, *J. Magn. Magn. Mater.* 321 (2009) 3278–3284.
- [31] Z.Y. Xu, B.G. Shen, *Sci. China Tech. Sci.* 55 (2012) 445–450.
- [32] B.K. Banerjee, *Phys. Lett.* 12 (1964) 16–17.
- [33] E. Talik, M. Kulpa, A. Winiarski, T. Mydlarz, M. Neumann, *J. Alloy. Comp.* 316 (2001) 51–57.
- [34] E. Talik, M. Kulpa, T. Mydlarz, J. Kusz, H. Böhm, *J. Alloy. Comp.* 348 (2003) 12–17.
- [35] J. Mira, J. Rivas, F. Rivadulla, C. Vázquez-Vázquez, M.A. López-Quintela, *Phys. Rev. B* 60 (1999) 2998–3001.
- [36] P. Sarkar, P. Mandal, A.K. Bera, S.M. Yusuf, L.S. Sharath Chandra, V. Ganesan, *Phys. Rev. B* 78 (2008) 012415.
- [37] N. Chau, D.H. Cuong, N.D. Tho, H.N. Nhat, N. H. Luong, B. T. Cong, *J. Magn. Magn. Mater.* 272–276 (2004) 1292–1294.
- [38] Z.D. Han, H.L. Wu, D.H. Wang, Z.H. Hua, C.L. Zhang, *J. Appl. Phys.* 100 (2006) 043908.
- [39] Q. Luo, B. Schwarz, N. Mattern, J. Eckert, *Phys. Rev. B* 82 (2010) 024204.
- [40] A.M. Tishin, Y.I. Spichkin, *The Magnetocaloric Effect and its Applications*, Institute of Physics Publishing, (2003) pp. 240–245.
- [41] B. Li, W. L. W. J Ren, W.J. Hu, J. Li, C.Q. Jin, Z.D. Zhang, *Appl. Phys. Lett.* 100 (2012) 242408.
- [42] J.S. Marcos, J.R. Fernández, B. Chevalier, J.L. Bobet, J. Etourneau, *J. Magn. Magn. Mater.* 272–276 (2004) 579–580.